# Wood-chip water content sensor with capacitance tomography

**Cédric Margo[1],Jérôme Lucas[1],Thierry Ditchi[2],Emmanuel Géron[1], Stéphane Holé [2,#] and Jacques Lewiner[1]**

1 Electrical Engineering Laboratory (LEG), ESPCI-ParisTech, 10 rue Vauquelin, 75005, Paris, France
2 Physics and Material Study Laboratory (LPEM), UPMC, ESPCI-ParisTech, CNRS 8213, 10 rue Vauquelin, 75005 Paris, France
# Corresponding Author / E-mail: stephane.hole@espci.fr, TEL: +33-140794571

KEYWORDS : Sustainable energy, Wood-chips, Water content, Moisture sensor, Capacitive Tomography, ECT

*Wood-chips are one of the best sources of sustainable energy. The potential sustainable production in France could reach nearly 10% of the overall country energy needs. Because energy efficiency of wood-chips is highly dependent on their water content, there is a need for a rapid, transportable and precise water content measurement system. In this paper we propose a capacitance tomographic approach to evaluate the water content of the wood-chips. Our system is based on a bucket equipped with 18 electrodes able to probe 6 liters of wood-chips. With adequate electrode polarizations and a highly efficient processing electronics, we have been able to obtain a repeatability of about 1%, which is compatible with wood-chip industry requirements.*

Manuscript received: January XX, 2011 / Accepted: January XX, 2011

**NOMENCLATURE**

ECT = Electrical Capacitance Tomography
P = Peripheral measurements
T = Transversal measurements

## 1. Introduction

The steadily increasing use of fossil fuels has lead to a significant rise in the amount of carbon dioxide ($CO_2$) in the atmosphere. Consequently, identifying suitable sustainable energy sources is extremely important for future generations [1]. Wood is a renewable energy source as burning it produces no more $CO_2$ than it has captured during its growth. Wood-chips are small pieces of wood of a few inches wide. They are particularly interesting as they are a wood source that would otherwise be thrown away, they are cheap and the energy needed to use them (shredding, transportation,...) is less than 3% of the energy they could provide during combustion. The potential sustainable production in France could reach nearly 10% of the overall country energy needs. This makes them one of the best sources of renewable energy, but this level of performance can only be achieved if the wood-chips are dry enough. Indeed, the presence of water in the wood actually reduces its energy value by mass as for the same mass, there is less wood and some of the energy supplied is used to vaporize the water. The energy efficiency of wood-chips is usually quantified by the net heating value which represents the theoretically available energy for the end user in Wh/kg. It is important to notice that water content of wood-chips has a great influence on their energy efficiency while the wood species used have only a little influence. Typically, the variation of the net heating value among all the common French wood species is at most +/- 3.5%, which corresponds to a water content increase of only 3.3 %. As a comparison, while three tons of wood-chips with 20% water content are equivalent to one ton of oil, two more tons are required to produce the same amount of energy with wood-chips having 50% water content. A freshly cut tree presents a water content as high as 60%. To allow forestry wood-chip industry to emerge one must be able to quantify the actual energy delivered to the consumer. This requires measuring the amount of water at each stage of the industrial supply chain, particularly at sites of storage, drying and delivery.

Usually, water content measurements are performed by drying up a sample of wood-chips in an oven at 103°C and comparing the weight of the sample before and after the drying up process. This is a precise but slow method, results being known the day after. Other methods have been proposed to perform water content measurements. Amongst them, capacitive measurements [2] are good candidates because they are rapid, robust and easy to perform. However, the capacitive systems currently available on the market remain unable to provide the 1% precision expected by wood-chip industries [3, 4].

In this paper we propose a new approach based on electrical capacitance tomography (ECT) to estimate the water content of wood-chips. The sensor consists of a 6-liter bucket equipped with 18 electrodes. After a description of the theoretical background, we show how it is possible to optimize the polarization scheme of the sensor by calculating its sensitivity map. Finally, the experimental results obtained with our sensor are presented and appear to be precise

enough to meet the wood-chip industry requirements.

## 2. Water content sensing in wood-chips

Capacitive sensing is a useful way to sense the water content in materials or even atmospheric hygrometry. Many kind of sensors have been used for this purpose, ranging from the classical parallel plates capacitor geometry to more complex coplanar interdigital structures [5, 6]. The reason for its use is that the relative permittivity of water is high (around 80) compared to common insulating materials (less than 5) [7]. Capacitive water content sensing actually consists of measuring the variation of relative permittivity of the material caused by a variation of water content. Fig. 1 shows the standard configuration using two opposite parallel electrodes to form a capacitor, the material being sensed acting as the dielectric of the capacitor.

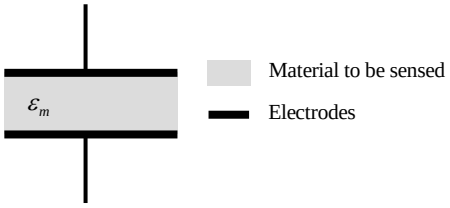


Fig. 1 The basic parallel plate capacitive sensor

In this basic configuration, the capacitance C is simply given by:

$$C = \varepsilon_m \cdot \varepsilon_0 \cdot \frac{S}{d} \tag{1}$$

Where $\varepsilon_m$ is the relative permittivity of the medium being sensed, $\varepsilon_0$ is the permittivity of vacuum, d is the thickness of the sample and $S$ the surface of the electrodes in contact with the sample. Considering a homogeneous material and a uniform distribution of the water in the medium, a variation of water content would give rise to an important variation of the relative permittivity and consequently to an easily measurable variation of capacitance, assuming that the thickness and surface of electrodes are correctly chosen. Nevertheless, one has to notice that this configuration is very sensitive to the shape and dimensions of the sample. Moreover, measuring water content of wood-chips is not as straightforward as in this simple case. Indeed, wood-chips consist of wood scraps of different size and shape. As a consequence, the material probed by the sensor is a heterogeneous mixture of air, dry and wet wood. Historically, many theoretical models have been proposed to estimate the equivalent homogeneous permittivity of a heterogeneous medium. One of the most famous is probably the Maxwell Garnett [8, 9] model which considers a uniform distribution of inclusion spheres having a permittivity $\varepsilon_i$ immerged in a host medium having a permittivity $\varepsilon_h$ (see Fig. 2). In such a case, the equivalent homogeneous permittivity $\varepsilon_e$ of the mixture can be estimated by:

$$\varepsilon_e = \varepsilon_h + 2 \cdot v \cdot \varepsilon_h \cdot \frac{\varepsilon_i - \varepsilon_h}{\varepsilon_i + \varepsilon_h - v \cdot (\varepsilon_i - \varepsilon_h)} \tag{2}$$

Where $\varepsilon_h$ stands for the permittivity of the homogeneous host medium, $\varepsilon_i$ is the permittivity of inclusion spheres, and $v$ is the volume fraction of inclusion spheres. Assuming a known host medium (air for instance) and a known volume fraction of inclusions, one can deduce the permittivity of the inclusion spheres, hence be directly sensitive to water content inside the spheres.

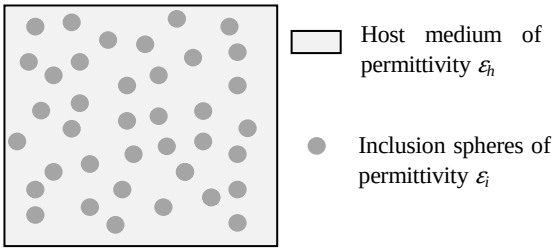


Fig. 2 Dielectric mixture used in the Maxwell Garnett model

This model assumes a very specific case where the shape, size and volume fraction of inclusions can be predicted, and that all the spheres have the same permittivity. Even if various extensions of this model have been developed over the years to account for more specific geometries, they are not easily applicable to the case of wood-chip samples for which size and shape of scraps can be very irregular. In addition, the position of the water in a wood-chip sample varies with each sample and even within a given sample. To be able to measure wood-chip water content, one must be able to render the measuring system as insensitive as possible to the position of the water in the sample.

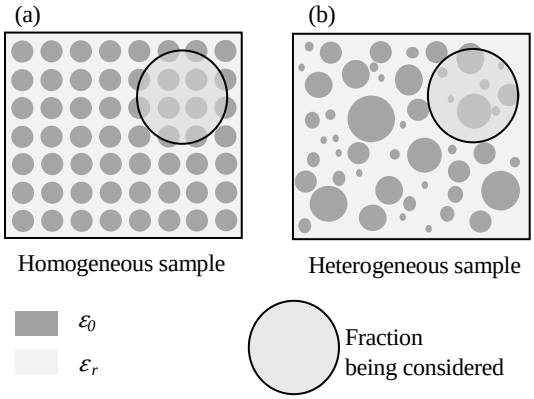


Fig.3 Statistical averaging - (a) uniform distribution (b) heterogeneous distribution

This could be achieved by considering a sufficiently large sample to allow statistical averaging as depicted in Fig. 3. In Fig. 3a the sample is homogeneous while in Fig. 3b it is heterogeneous. However both samples contain the same fraction of wood (with water) and air. Therefore, the measuring system should detect the same water content. But errors can arise if the probed volume is reduced. Electrical capacitance tomography (ECT) can be used to obtain position dependant information. In our case, it is interesting to determine permittivity at the center of the sample and at its periphery to avoid boundary effects. For that purpose, it is necessary to estimate the sensitivity map of the sensor.

## 2. Capacitive sensors

Generally speaking, capacitive sensors can be seen as set of electrodes in contact with dielectric materials. Electrodes are the terminals and dielectrics can be mechanical parts of the sensor or a material under measurement. Fig. 4 illustrates a generic description of such a capacitive sensor with four electrodes, one being at infinity (electrode 4). The sensor is operated by polarizing one or more of its

electrodes (driven electrodes), and measuring the corresponding charges appearing on the electrodes. The measured capacitances depend on the electrode polarization scheme, the permittivity distribution, and the shape and position of electrodes.

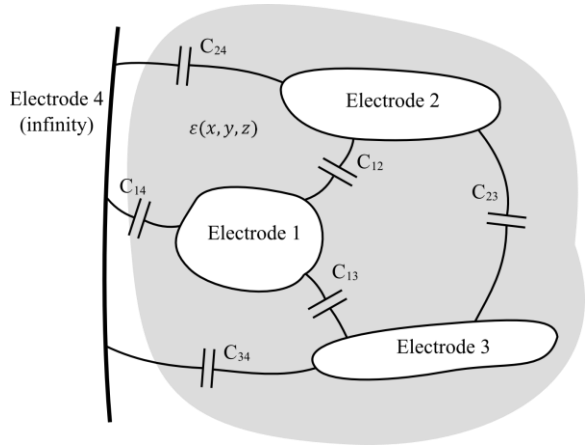


Fig. 4 A generic capacitive sensor

It is common to describe a multi-electrodes capacitive sensor with the capacitive tensor which links the potential on the electrodes to the charges they hold. For instance, considering the capacitive sensor depicted in Fig. 4, the relation between the potential on the electrodes and their charges is given by:

$$\begin{bmatrix} Q_1 \\ Q_2 \\ Q_3 \\ Q_4 \end{bmatrix} = \begin{bmatrix} \sum C_{1j} & -C_{12} & -C_{13} & -C_{14} \\ -C_{12} & \sum C_{2j} & -C_{23} & -C_{24} \\ -C_{13} & -C_{13} & \sum C_{3j} & -C_{34} \\ -C_{14} & -C_{24} & -C_{34} & \sum C_{4j} \end{bmatrix} \begin{bmatrix} V_1 \\ V_2 \\ V_3 \\ 0 \end{bmatrix} \quad (3)$$

Where $Q_i$ is the quantity of charges on electrode $i$ and $V_i$ its potential. Coefficients $C_{ij}$ are the inter-electrodes capacitances. In others words, they represent the amount of charges on electrode $i$ when all electrodes are held to 1 V except electrode $j$ which is grounded. Not all coefficients are independent in the capacitive tensor. Indeed for a $N$-electrode configuration (including electrode at infinity), the number of independent capacitance measurements that can be carried out is at most $N(N-1)/2$.

## 3. Capacitance tomography

### 3.1 General description

Capacitance tomography is an application of capacitive sensing. Its aim is to reconstruct a cross-section image of a dielectric material from multiple inter-electrode-capacitance measurements. The dielectric material can present a homogeneous or heterogeneous permittivity distribution but, in a typical case the permittivity distribution is heterogeneous and the aim of the so called capacitance tomography is to reconstruct an image of the permittivity distribution in the sample. Fig. 5 illustrates a basic tomographic sensor. It consists of a cylinder surrounded here by 8 electrodes, but can be extended to $N$ electrodes. Even if capacitance tomography systems are not restricted to this geometry, it is the most commonly used, typically for monitoring fluids flowing through a pipe [10]. That is actually the geometry that has been used for our sensor.

Each electrode can be independently polarized and the charges can be measured on any of the 8 electrodes. The number of independent measurements is then 28 at most. This relatively high number of independent measurements allows summing up equivalent measurements to gain in statistics considering the symmetry of the sample.

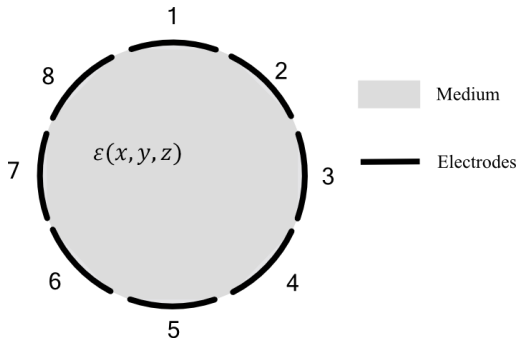


Fig. 5 A typical capacitance tomography sensor configuration

### 3.2 Sensitivity map

In capacitance tomography, sensitivity map is a keystone to image reconstruction. It is required to build up the permittivity distribution from the inter-electrode-capacitance measurements. Many approaches exist to build the sensitivity map of a tomographic capacitance sensor. Some of them are based on linear approximations. For instance, one can consider a subdivision of the domain into a finite number of elements, and obtain the response of the sensor as a linear sum of responses when the permittivity of one element varies [11]. Whatever the electronic method used for measuring inter-electrode capacitances, the measurement is always equivalent to a charge measurement. Therefore the sensitivity can be defined as an elementary charge variation $\delta Q_m$ on the electrode used for measurement corresponding to an elementary spatial variation of permittivity $\delta\varepsilon$ in the probed volume. Before the permittivity variation $\delta\varepsilon$, the electrostatic equilibrium is given by the Gauss equation:

$$div(\varepsilon\vec{E}) = 0 \quad (4)$$

The variation of permittivity at one position in space leads to a variation of the electric field in the sensor structure and of the charges of the electrodes. So, if $\varepsilon$ becomes $\varepsilon + \delta\varepsilon$, the electric field $\vec{E}$ becomes $\vec{E} + \delta\vec{E}$. The new electrostatic equilibrium resulting from the variation of permittivity is thus given by:

$$div\left((\varepsilon + \delta\varepsilon)(\vec{E} + \delta\vec{E})\right) = 0 \quad (5)$$

Neglecting second-order terms and subtracting the two electrostatic equilibria given respectively by equations (5) and (4) (before and after the permittivity variation), one obtains:

$$div\left(\varepsilon\delta\vec{E} + \delta\varepsilon\vec{E}\right) = 0 \quad (6)$$

Equation (6) represents an equivalent electrostatic equilibrium deriving from those before and after the permittivity variation. In short-circuit measuring condition all electrodes are grounded in this equivalent equilibrium since there was no voltage variation between (4) and (5) and the charge $\delta Q$ on the electrodes and the electric field $\delta\vec{E}$ in the sensor are only generated by the equivalent permanently oriented dipole distribution $\delta\varepsilon\vec{E}$.

The variation of charge on electrode $m$ $\delta Q_m$ can be more easily calculated if we determine the contribution $\delta q_m$ of a unique punctual

dipole $\vec{p}$ at an arbitrary position $\vec{x}$ and then integrate $\delta q_m$ over the contribution of all the dipoles of the distribution $\delta\varepsilon\vec{E}$. According to Coulomb's law, a punctual dipole can be seen as a couple of charges of strength $q$, of opposite polarity and separated by a distance $\vec{l}$ :

$$\vec{p} = q \cdot \vec{l} \tag{7}$$

The Gauss identity provides a simple way to calculate $\delta q_m$. It connects two electrostatic equilibria $A$ and $B$ by:

$$\int V_A \cdot \rho_B \cdot dv = \int V_B \cdot \rho_A \cdot dv \tag{8}$$

where $V_A$ and $\rho_A$ are respectively the potential and charge density of the first equilibrium $A$, and $V_B$ and $\rho_B$ the potential and charge density of equilibrium $B$. Equilibrium $A$ corresponds to the electrostatic equilibrium given by equation (6) in which the dipole density $\delta\varepsilon\vec{E}$ is replaced by a punctual dipole $\vec{p}$ . In the electrostatic equilibrium $B$, all electrodes are grounded except the measuring electrode which is held at a potential $V_{Bm}$. In this situation, the first member of (8) is zero since charges $\rho_B$ are located only on the electrodes and $V_A$ is null on all electrodes. In equilibrium $A$, charges are located on the electrodes but also at the position of the punctual dipole. So, the second member of the Gauss identity (8) is:

$$\int V_B \cdot \rho_A \cdot dv = V_{Bm}\delta q_m + q\left(V_B(\vec{x}+\vec{l}/2) - V_B(\vec{x}-\vec{l}/2)\right) \tag{9}$$

since $V_B$ is zero on all electrodes except the measuring electrode for which $V_B = V_{Bm}$. Considering moreover that electric field derives from potential, one gets from Gauss identity:

$$V_{Bm}\delta q_m = -q\vec{l}\cdot\vec{grad}(V_B)(\vec{x}) = \vec{\rho}\cdot\vec{E}_B(\vec{x}) \tag{10}$$

where $\vec{E}_B$ is this electric field in equilibrium state $B$. It also corresponds to the electric field in the sensor structure when the measuring electrode is held to $V_{Bm}$ and other electrodes are grounded. One can define therefore $\vec{\xi}_m$ as:

$$\vec{\xi}_m = \frac{\vec{E}_B}{V_{Bm}} \tag{11}$$

and considering $\vec{p} = \delta\varepsilon\vec{E}dv$ , one obtains finally by integrating over space, the sensitivity [12, 13]:

$$\delta Q_m = \int \delta q_m = \int \delta\varepsilon\,\vec{E}\cdot\vec{\xi}_m\,dv \tag{12}$$

It should be reminded that $\vec{E}$ is the electric field in the probed volume resulting from the polarization of the electrodes before the permittivity variation $\delta\varepsilon$, $\vec{\xi}_m$ is the electric field produced by the electrode on which the charges are measured when it is held to 1 V while all other electrodes are grounded. The field $\vec{\xi}_m$ can be called the sensitivity field. The integral should be calculated over all positions where permittivity can vary. Practically, this can be limited to the probed volume, that is to say where the permittivity can vary.

Equation (12) can be used to calculate the sensitivity map of any kind of electrode configuration. Typically, for a given electrode configuration, one can first estimate the electric-field distribution using a finite-element software, and then calculate the sensitivity map using equation (12). In this way, the morphology of the sensor (size, shape and number of electrodes) and the polarization scheme can be chosen to optimize the sensor sensitivity map.

Note that, in the case of water content estimation in a wood-chip sample, image reconstruction is not the final goal. Indeed, the sensitivity map would rather be used as a tool to optimize the statistical averaging of inter-electrode-capacitance measurements. Let for example consider the basic tomographic sensor illustrated in Fig. 5. For this configuration, we have calculated the sensitivity map for some specific cases. Indeed, we consider two situations:

-Peripheral measurements (P) for which one electrode is polarized while all others are grounded. The charge is measured at the polarized electrode. The relative sensitivity map for this configuration is illustrated on Fig. 6a (in log scale) where electrode 8 is polarized.

-Transversal measurements (T), for which two opposite electrodes are used, one for polarization and one for measurement. This is illustrated in Fig. 6b (in linear scale) for which electrode 8 is polarized and charges are measured on electrode 4.

It is shown that the sensitivity is quite large near to the electrodes in the case of a peripheral measurement (Fig. 6a) but does not penetrate into the sample, while a good penetration depth is observed for the transversal measurement (Fig. 6b) but the sensitivity remains low, even in the close proximity of electrodes.

The sensitivity map can be optimized using statistical averaging, owing to cylindrical geometry. This is shown in Fig. 6c and Fig. 6d (both in log scale) for which the sensitivity map is calculated by summing up all signals obtained from peripheral measurements for Fig. 6c, and from transversal measurements for Fig. 6d. Those configurations give rise to a greater sensitivity and tend to homogenize the sensitivity map in the middle of the sample.

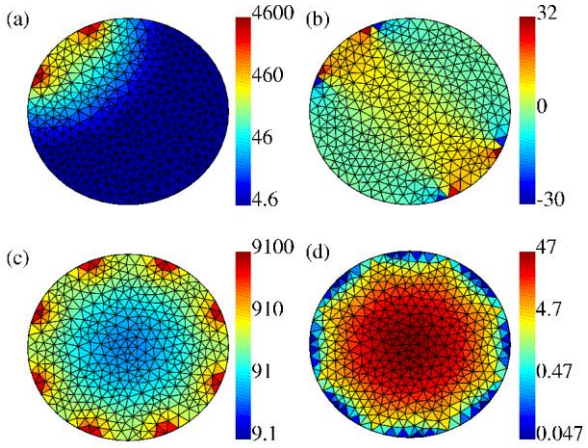


Fig. 6 Relative sensitivity map for different polarization schemes (a) Peripheral (one electrode) (b) Transversal (two opposite electrodes) (c) sum of all peripheral configurations over all angles (d) sum of all transversal configurations over all angles.

## 3. Experimental set-up and results

The experimental set-up for measuring wood-chip water content consists of a cylinder surrounded by 18 electrodes, into which a bucket filled with 6 liters of wood-chips is inserted (see Fig. 7). The electrodes are more widely spaced than in the theoretical study presented in the previous section. This reduces the sensitivity in regions close to electrodes and increases it in the middle of the sample according to theoretical calculations (Fig. 6). The whole measurement system was connected to a charge-transfer based electronic circuit developed for the application, and able to measure capacitances of a fraction of picofarads connected at the end of

coaxial wires whose capacitance is typically worth a few nanofarads.

The electronic circuit has been programmed to perform successively peripheral and transversal measurements as described in section 3.2. According to Fig. 6, peripheral measurements give a better sensitivity at the bucket periphery while transversal measurements are almost homogeneously sensitive in the middle of the bucket. Fig. 8 shows the results obtained by summing up all peripheral measurements (referred to as P on Fig. 8), and all transversal measurements (referred to as T on Fig. 8) for different water contents. For each water content, 6 measurements were performed with different wood-chips spatial arrangements in order to check the repeatability of the system.

Fig. 7 Experimental set-up: bucket filled with wood-chips (left side) and measurement cylinder with electrodes (right side)

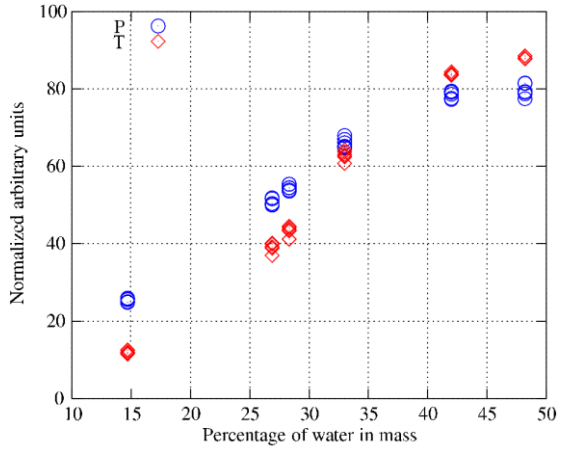


Fig. 8 Experimental results – Peripheral (circles) and transversal (diamonds) measurements versus water content

The different water contents values were obtained by drying up a fraction of the sample in an oven between each measurement. From Fig. 8, it can be seen that peripheral (P) and transversal (T) measurements significantly vary with water content while signal variation between re-arranged samples for a given water content is very low. These results show the good sensitivity of the sensor to water content. If we consider the dispersion of the different measurements for each water content, we can estimate the relative precision of our sensor. The precisions for different water contents are summarized in Table 1.

| % water | 14.7 | 26.9 | 28.3 | 33 | 42 | 48.2 |
|---|---|---|---|---|---|---|
| %error in P | 0.9 | 0.6 | 0.6 | 1 | 2.6 | 5 |
| %error in T | 0.9 | 1 | 1.2 | 2.2 | 1.1 | 1 |

Table 1 Precision of the sensor for different water contents

According to Table 1, the precision obtained remains lower than 2.6% over the whole water content range. It is even lower than the required 1% by wood-chip industries at low water content for which the maximal precision is required for delivery. Concerning the measurements dependence with water content, one can see on Fig. 8 that, for low water contents, both peripheral and transversal measurements tend to increase linearly with water content. At higher water content (above 35%), peripheral and transversal measurements seem to behave in a different way. By using an appropriate signal processing strategy, one could get more relevant information from these two different trends.

## 4. Conclusion

We have proposed a new approach based on capacitance tomography to estimate quickly and efficiently the water content of wood-chips. Unlike traditional capacitance measurements, the tomographic-like approach allows a better statistical averaging of measurements and is almost insensitive to wood-chips spatial arrangement in the sample. The precision obtained meets the requirements of wood-chip industry, that is to say 1%.

## ACKNOWLEDGEMENT

This work has been supported by ADEME and ANR during OMICAGE Project. We thank UCFF for having provided all wood-chip samples.

## REFERENCES

1. Fortunat Joos et al., “Global warming feedbacks on terrestrial carbon uptake under the intergovernmental pane on climate change (IPCC) emission scenarios.” *Global Biochemical Cycles*, Vol. 15, pp. 891-907, December 2001.

2. Robert Puers. “Capacitive sensors: when and how to use them.” *Sensors and actuators A*, Vol. 37-38, pp. 93-105, 1993.

3. Jensen PD, Hartmann H, Bohm T, et al., “Moisture content determination in solid biofuels by dielectric and NIR reflection methods”, Biomass & Energy, Vol. 30, No. 11, pp. 935-943, 2006.

4. Hartmann H., Böhm T., “Rapid moisture content determination of wood chips – results from comparative trials”, Proceedings 1st Wolrl Conference on Biomass for Energy and Industry, 5-9 June in Sevilla, James & James Ltd., London, 2001, pp. 571-574.

5. Bhuiyan R.H., Dougal R.A., Ali M., “Proximity coupled interdigitated sensors to detect insulation damage in power system cables”, Sensors Journal, IEEE, Vol. 7, No .12, ISSN 1530-437X, 2007.

6. Alexander V. M., Kishore S. R., Fumin Y., Yanqing D., Markus. Z, ”Interdigital Sensors and Transducers”, Proceedings of the

IEEE, Vol. 92, N0. 5, 2004.

7. Hasted. J.B., "Liquid water: Dielectric properties." In F. Franks, editor, *Water: A comprehensive treatise*, Vol. 1, pp. 255-309. PlenumPress, USA, 1972. ASIN: 0306371855.
8. Karkkainen K.K., Sihvola, A.H., Nikoskinen K.I., "Effective permittivity of mixtures: numerical validation by the FDTD method" , Vol. 38, No. 3, pp. 1303-1308, 2000.
9. Maxwell Garnett J. C., Colours in Metal Glasses and in Metallic Films, Phil. Trans. R. Soc. Lond. A, 1904.
10. Wang F., Marashdeh Q., Fan L. S., Warsito W., "Electrical Capacitance Volume Tomography: Design and Applications", Sensors, Vol. 10, No. 3, pp 1890-1917, 2010.
11. Marashdeh Q., "Advances in electrical capacitance tomography", dissertation, Ohio State University,2006.
12. Lucas J., Holé S., Bâtis C., "Analytical capacitive sensor sensitivity distribution and applications", Meas. Sci. Technol., Vol. 17, pp 2767-2478, 2006.
13. Lucas J., Holé S., Bâtis C., "Simple and direct calculation of capacitive sensor sensitivity map", COMPEL, Vol. 27, pp. 307-318, 2008.